UDC 52-323.8
Doi: 10.31772/2712-8970-2023-24-3-537-549

Для цитирования: Лукьянов М. М., Зуев Д. М. Рассмотрение возможности стабилизации относительного движения наноспутников под действием активного аэродинамического управления // Сибирский аэрокосмический журнал. 2023. Т. 24, № 3. С. 537–549. Doi: 10.31772/2712-8970-2023-24-3-537-549.

For citation: Lukyanov M. M., Zuev D. M. [Estimation of the possibility of matching the relative motion of nanosatellites under active aerodynamic control]. *Siberian Aerospace Journal.* 2023, Vol. 24, No. 3, P. 537–549. Doi: 10.31772/2712-8970-2023-24-3-537-549.

Рассмотрение возможности стабилизации относительного движения наноспутников под действием активного аэродинамического управления

М. М. Лукьянов*, Д. М. Зуев

Сибирский государственный университет науки и технологий имени академика М. Ф. Решетнева
Российская Федерация, 660037, г. Красноярск, просп. им. газ. «Красноярский Рабочий», 31
*E-mail: mishka.1255555@mail.ru

В статье рассмотрены перспективы применения аэродинамического управления для поддержания формации наноспутников класса CubeSat. Целью данной работы является оценка границ применения активного аэродинамического контроля для стабилизации относительного движения двух аппаратов CubeSat 3U на солнечно-синхронной орбите высотой 570 км. Проведен обзор теоретических сведений об аэродинамических силах, действующих на искусственные спутники Земли, в рамках которого рассмотрены модели верхней атмосферы Земли. Рассмотрены аспекты построения дифференциальной силы лобового сопротивления для наноспутников в качестве исполнительного механизма активного управления. Для исследования орбитального движения спутников под действием аэродинамического управления с помощью программы General Mission Analysis Tool смоделирован групповой полет двух космических аппаратов с учетом факторов, вызывающих возмущения орбит. По результатам экспериментов изучена динамика межспутникового расстояния и сделан вывод о возможности применения аэродинамической дифференциальной силы для стабилизации относительного движения.

Ключевые слова: CubeSat, групповой полет, дифференциальная сила, аэродинамическое сопротивление, GMAT.

Estimation of the possibility of matching the relative motion of nanosatellites under active aerodynamic control

M. M. Lukyanov*, D. M. Zuev

Reshetnev Siberian State University of Science and Technology
31, Krasnoyarskii Rabochii prospekt, Krasnoyarsk, 660037, Russian Federation
*E-mail: mishka.1255555@mail.ru

The article discusses the prospects of utilization of aerodynamic control to maintain the formation of nanosatellites of the CubeSat class. The purpose of this work is to estimate the limits of the application of active aerodynamic control to stabilize the relative motion of two CubeSat 3U satellites in a sun-synchronous orbit with a height of 570 km. A review of theoretical information about aerodynamic forces acting on artificial Earth satellites is carried out, within the framework of which models of the Earth's up-

per atmosphere are considered. Aspects of creating a differential drag force for nanosatellites as an active control actuating mechanism are considered. To study the orbital motion of satellites under the action of aerodynamic control using the General Mission Analysis Tool program, a group flight of two spacecraft was simulated taking into account the factors causing orbital disturbances. Based on the results of experiments, the dynamics of the inter-satellite distance was studied, and a conclusion was made about the possibility of using an aerodynamic differential force to achieve a stable relative motion.

Keywords: CubeSat, formation flight, differential force, aerodynamic drag, GMAT.

Introduction

For space missions that involve multiple satellites sharing a common infrastructure, NASA has coined the term “multi-satellite.” Currently, multi-satellite missions are gaining popularity in the rocket and space industry. They make it possible to solve a wide range of tasks that cannot be performed using a single device. Small space vehicles (SSV), such as nanosatellites of the CubeSat class [1], are suitable for building multi-satellite configurations in orbit due to the presence of a unified platform and low cost of production and launch [2]. A group of small satellites can be considered as a profitable alternative to a larger and more expensive device for use in such areas as remote sensing of the Earth, studying the upper layers of the atmosphere, studying the radiation situation and conducting other scientific experiments, as well as the deployment of synthetic aperture antenna systems [3; 4].

Missions that involve multiple satellites can be divided into two categories: constellation missions and formation flying missions [5]. The use of satellite constellations allows providing the greatest coverage of the Earth. In this case, the position of each satellite is controlled separately relative to a given point. Constellations of spacecraft (SC) are divided into controlled ones, in which each satellite actively maintains its position (for example, GLONASS), and uncontrolled, in which there is no active control over the position of the satellites. Unlike constellations, satellite formations require control of the inter-satellite distance, as well as the relative orientation of the spacecraft. The construction of the formation is hampered by disturbances in satellite orbits caused by the influence of the nonsphericity of the Earth’s gravitational potential, atmospheric resistance, the pressure of solar radiation and the gravitational attraction of other bodies [6]. These disturbances can cause the satellites to rapidly move away from each other.

Traditional flight control systems allow a communication session with a spacecraft only when it is within the radio visibility zone of one of the available ground stations. Therefore, most of the flight time there is no connection with the device. One of the options for solving this problem is to organize an inter-satellite radio link in the architecture of the communication system. With a sufficient number of satellites in the formation, it is possible to provide a round-the-clock communication line between the ground complex and any spacecraft. Formations with inter-satellite communication make it possible to reduce delays in accessing information to the consumer and provide access to real-time information services [7]. To implement radio communication sessions between satellites, it is necessary to keep them at a certain distance, at which it will be possible to transmit a signal from one satellite to another. In the context of this problem, the need to use active means of inter-satellite distance control is most clearly expressed.

Formation and maintenance of formations in orbit can be carried out using propulsion systems (PS). However, in the case of CubeSat devices, their use turns out to be difficult due to strict restrictions on the mass, volume and power of the CubeSat platform [8].

An alternative is aerodynamic control of relative motion, performed by the difference in drag forces applied to the satellites. This difference in forces, called differential force, is provided by changing the orientation of the spacecraft relative to its velocity vector and, consequently, changing its cross section (midsection). The advantages of aerodynamic control are the absence of the need for fuel consumption, low risks of mechanical damage, as well as the low cost of implementing relatively expensive remote control systems.

The purpose of this work is to assess the limits of using active aerodynamic control to maintain a formation consisting of two CubeSat-class devices with a 3U form factor in orbit at an altitude of 570 km.

Physical foundations of aerodynamics of orbital motion of spacecraft

The aerodynamic impact experienced by satellites in low Earth orbit (LEO) can be divided into two components: the drag force directed against the velocity vector and the so-called lift force, perpendicular to the planes that the atmospheric molecules collide with (Fig. 1) [9].

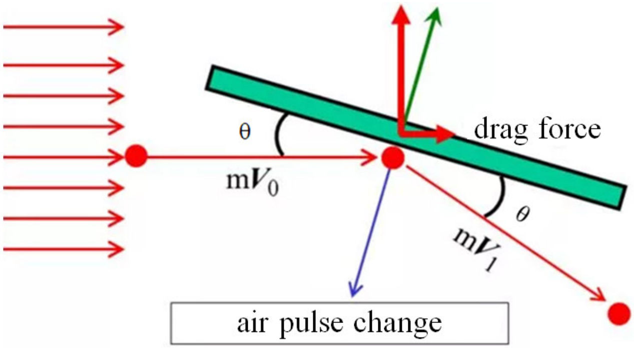

Рис. 1. Аэродинамические силы, действующие на тонкую пластину [10]

Fig. 1. Aerodynamic forces acting on a thin plate [10]

Low atmospheric resistance is a constantly acting force and, over a long period of time, can significantly change the orbital parameters of an artificial Earth satellite (AES). The drag force can be expressed in the direction opposite to the satellite’s speed $\vec{v}$:

$$F_{drag} = ma_{drag} = -\frac{1}{2}\rho C_D A_{ref} |\vec{v}|^2 , \tag{1}$$

where ρ is the atmospheric density; m is the mass of the satellite; C_D is a drag coefficient; A_{ref} is a reference midship area of the satellite.

Formula (2) says that the aerodynamic drag force depends on the parameters determined by the altitude of the orbit (atmospheric density and free-stream velocity), as well as on the ballistic parameters of the satellite. These include the mass of the satellite, as well as its drag coefficient and midship area, which are determined by the shape of the vehicle and its orientation relative to the oncoming flow. It is convenient to represent them in the form of a ballistic coefficient:

$$B_C = \frac{m}{C_D A_{ref}} . \tag{2}$$

Dividing the parts of equation (2) by the mass of the satellite and expressing its ballistic parameters through the ballistic coefficient, we write the expression for the acceleration caused by the drag force can be written in the following way:

$$a_{drag} = -\frac{\rho |\vec{v}|^2}{2B_C} . \tag{3}$$

Thus, the lower the ballistic coefficient is, the greater the impact of atmospheric braking on a spacecraft is. Taking into account the value of this parameter when designing the shape of the spacecraft and its mass will make it possible to determine the magnitude of the aerodynamic impact exerted on it.

Various models are used to determine the atmospheric density ρ. They can be implemented for both numerical and approximate analytical calculations in the vicinity of the reference height. These standards determine the density of the atmosphere depending on a given time, orbital altitude, latitude and longitude, as well as the level of solar activity, which affects the parameters of the upper layers of the earth's atmosphere [11]. Models of the upper atmosphere include latitudinal, seasonal, geomagnetic and solar effects. Variations in atmospheric resistance are taken into account, including the effects of diurnal variations, the Earth's tilt, the 27-day solar cycle (related to its rotation period), the 11-year solar cycle, semi-annual and seasonal variations, and cyclic variations in the 11th solar cycle.

Jacchia models are widely used in the space industry. The database underlying Jacchia consists of tabulated empirical profiles of temperature, composition, density and pressure as a function of altitude ranging from 90 to 2500 km [12]. The Jacchia model is based on satellite accelerometer data as well as drag data obtained from ground tracking of various satellites.

Models of the MSIS (Mass Spectrometer-Incoherent Scatter Radar) class [13] are based on data on the composition, temperature and total mass density of the upper atmosphere accumulated over a period of more than twenty years. The instruments used to study the composition of the atmosphere and its temperature were, respectively, a satellite mass spectrometer and ground-based incoherent scatter radar. Model NRLMSISE-00 is the latest model from the MSIS class [14]. This modification combines the advantages of both its predecessors from the MSIS class and the Jacchia models by combining and supplementing the database on which they are based.

GOST R 25645.166–2004 is based on data on the drag of artificial satellites [15]. It uses a simple analytical formula for calculations with coefficients expressing changes in atmospheric density during the solar cycle, daily fluctuations in solar activity and the geomagnetic index. The coefficients are tabulated for different levels of solar radiation flux. This standard also provides recommendations for using the model for ballistic tracking of satellites and a methodology for calculating the aerodynamic drag coefficient.

To simplify the expression for lift, it is assumed that the satellite has a thin braking surface much larger than the rest of the CubeSat shape, thereby ignoring the contribution of the body to the aerodynamic forcing on the satellite. In this case, the lift force can be expressed in a direction perpendicular to the brake plate and depending on its orientation:

$$F_{lift} = ma_{lift} = -\frac{1}{2}\rho C_L A_{ref} \left|\vec{v}\right|^2, \tag{4}$$

where C_L is the lift coefficient.

In LEO, the interaction of air with the satellite is such that the maximum value of the drag force is almost an order of magnitude greater than the value of the lift force [9]. First of all, this is due to the fact that the rotation of the apparatus negates the influence of the lifting force. In addition, satellites with a certain symmetrical shape will tend to cancel out the effect of aerodynamic lift. And furthermore, the lift coefficient is typically much smaller than the drag coefficient, which also makes the lift effect negligible in most cases. Therefore, as a rule, it is neglected when developing control algorithms. However, this leads to the loss of the potential ability to control motion outside the orbital plane.

Aerodynamic coefficients cannot be measured accurately in orbit. In addition, drag and lift coefficients for complex shapes are difficult to calculate analytically. To determine the values of these coefficients, a finite plate element method has been developed. To determine the values of these coefficients, a finite plate element method has been developed. Its essence lies in the decomposition of the complex shape of the satellite on the components of simple forms, assessing the impact of aerodynamic forces on each individual element and summing up the considered impact effects. The characteristics of planar elements are modeled using either experimental data, or theoretical models based on hypersonic interactions between gas and surface. For this method to be useful, the configuration of the spacecraft and its orbit must be determined.

Aerodynamic coefficients for simple planar elements can be estimated using physical models of gas-surface interaction, which gives different results depending on model assumptions. In the past, aerodynamic coefficients for simple shapes were calculated using the hyperthermal approximation. It assumes that the thermal speed of gas molecules is negligible. However, at altitudes from 120 to 600 km, the average thermal speed is comparable to the orbital speed. Later, aerodynamic drag and lift were considered using the theory of molecular free flow [16]. The drag and lift coefficients can be modeled for a simple thin plate using this theory:

$$C_D = 2\left[1 + \frac{2}{3}\sqrt{1 + \alpha\left(\frac{T_W}{T_\alpha} - 1\right)}\cos\theta\right], \tag{5}$$

$$C_L = \frac{4}{3}\sqrt{1 + \alpha\left(\frac{T_W}{T_\alpha} - 1\right)}\sin\theta, \tag{6}$$

where α is the accommodation coefficient; T_α is the temperature of the local atmosphere; T_w is the plate surface temperature; θ is the angle of incidence of the gas flow relative to the plate.

The accommodation coefficient α is a parameter that is used to take into account some important aspects of the chemical interaction of incoming air molecules with the surface of the spacecraft and is defined as

$$\alpha = \frac{E_{inc} - E_r}{E_{inc} - E_s}, \tag{7}$$

where E_{inc} is the kinetic energy of the falling molecule; E_r is the kinetic energy of the reflected molecule; E_s is the kinetic energy of reflected particles if they were emitted with the energy determined by the temperature of the satellite's surface.

Under conditions of free molecular flow, C_D weakly depends on the shape of the satellite and is determined mainly by the nature of the reflection of air molecules from the surface, $C_D \approx 2...2.5$. A reasonable drag coefficient value is 2.2 for a typical spacecraft. The drag coefficient depends on the shape of the satellite and the nature of the collision of air molecules with it. However, for estimates of long-duration orbital lifespan, the change in C_D with orbital altitude can safely be ignored since the percentage error in orbital lifespan will be quite small due to averaging effects around the assumed value of 2.2.

Relative motion of satellites under the influence of differential force

The differential force of aerodynamic drag is the difference in atmospheric drag forces acting on each of a pair of spacecraft. If satellites move through the atmosphere with the same density, then any differential drag is due to the difference in the ballistic coefficients of the vehicles in question.

This section examines a pair of satellites moving in close, low, circular orbits around the Earth. Typically, when analyzing relative motion, it is assumed that the satellites have the same shape with some flat part acting as a braking plate. An example of such a plane can be solar panels, as well as other deployable mechanisms. Due to rotation relative to the center of mass, the cross-sectional area of the spacecraft relative to the oncoming flow changes, this determines the magnitude of the aerodynamic force acting on it. If the satellites have different orientations relative to the oncoming flow, then a difference arises between the forces acting on the satellites.

Since CubeSat 3U class nanosatellites are parallelepiped-shaped, changing its orientation also changes the amount of drag, even in the absence of deployable plates. Thus, by changing the relative orientation, for example, using flywheels installed on board, it is possible to control the relative mo-

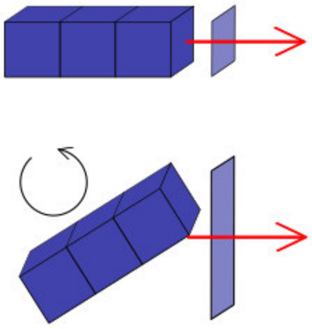

Рис. 2. Изменение площади миделя при изменении ориентации CubeSat

Fig. 2. Changing the midsection area when changing the orientation of the CubeSat

tion of the satellites' centers of mass. The differential force of aerodynamic drag will be determined by the difference in the effective cross-sectional area of the vehicles, which can be achieved due to different orientations of the satellites relative to the direction of movement (and the oncoming air flow, respectively). CubeSat 3U has dimensions of approximately 34.5 × 10 × 10 cm. Accordingly, its end faces have an area of 100 cm^2, and its side faces – 100 cm^2. The minimum drag force can be achieved by orienting such a nanosatellite along its velocity vector. In this case, the midsection area will be equal to the area of the end face (Fig. 2).

In the absence of orientation control, the average cross-sectional area is calculated, assuming that the position of the spacecraft can change uniformly relative to the direction of velocity. For a parallelepiped-shaped satellite, the average area can be calculated using the formula [17]:

$$CSA = \frac{1}{2}\left(S_1 + S_2 + S_3\right), \tag{8}$$

where CSA is the average cross-sectional area; S_1, S_2, S_3 are the areas of the sides of the device.

Substituting the areas of the end and two side faces of CubeSat 3U into formula (8), it can be determined that the effective cross-sectional area of such a satellite will be 390 cm^2.

Analysis of existing missions using aerodynamic control

To date, there is experience from several large missions that have used aerodynamic control as the only means of positioning satellites along the same orbit and keeping them at the required relative distances.

The Flock-1 satellite constellation [18], developed by Planet Labs Inc., consists of more than 100 CubeSats with a 3U form factor. These satellites provide high-resolution images of the Earth. 28 Flock-1 satellites were launched into low Earth orbit (400 km altitude, 52° inclination) from the International Space Station's NanoRacks CubeSat Deployer launch platform in mid-February 2014.

Relative motion control is achieved by modulating the background orientation of the satellites when they are not imaging or communicating with a ground station. Controlling the orientation of solar panels relative to the oncoming flow allows adjusting the cross-sectional area and provide a differential control force. Different attitude modes give different ballistic coefficients, different rates of aerodynamic orbital descent, and therefore different rates of mean motion acceleration. By controlling the amount of time each companion spends in the high-drag regime, it can be guaranteed that all satellites will end up moving the same way, resulting in zero relative velocity. By adjusting the timing of high-drag maneuvers, each satellite can be aimed at the desired orbital spacing relative to its neighbors.

Unlike pulse thruster control, satellite orbital positioning is limited by differential drag, since only the rate of descent is effectively modulated. The nominal low and high drag modes correspond to edges b and c, respectively, in Fig. 3, perpendicular to the velocity vector.

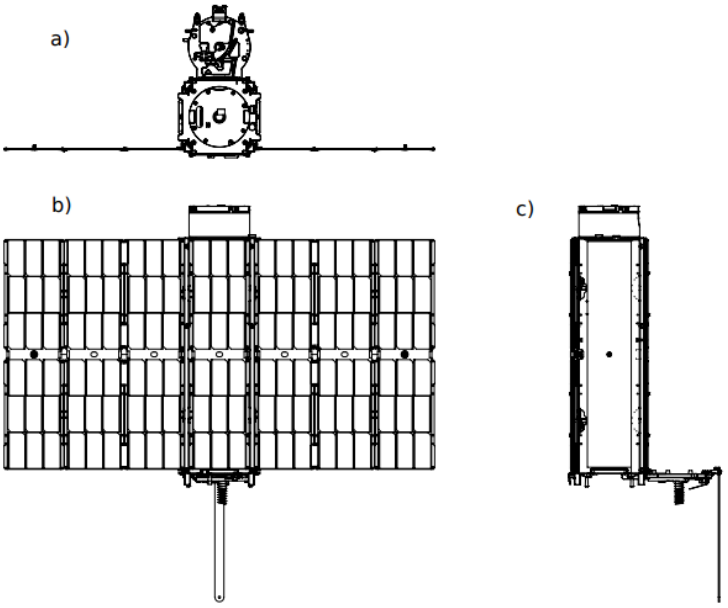

Рис. 3. Виды спутника Planet Labs Dove при обращении к встречному потоку:
a – камерой (200 см^2); *b* – солнечными панелями (1950 см^2); *c* – боковой панелью (370 см^2) [18]

Fig. 3. Types of the Planet Labs Dove satellite when addressing the oncoming flow:
a – camera (200 cm^2); *b* – solar panels (1950 cm^2); *c* – side panel (370 cm^2)

These modes result in an approximate midsection area ratio of 5:1. Control capabilities for this arrangement are highly dependent on orbital altitude and atmospheric conditions, but range from ≈ 1 km/day^2 in a 600 km sun-synchronous orbit to ≈ 50 km/day^2 or more in a 400 km orbit below the ISS.

The AeroCube-6 mission [19] is a pair of satellites launched into an elliptical sun-synchronous orbit at an altitude of 620–700 km on June 19, 2014. The satellites, having a 0.5U form factor, are equipped with two deployable panels (Fig. 4).

These spacecraft use aerodynamic control to regulate satellite altitude and inter-satellite distance. The orientation system is equipped with magnetic coils. The satellites were launched as a single package similar to 1U in size, and their separation occurred already during orbital movement. According to Fig. 3, the initial speed of the relative divergence of the satellites was 12 km/day (about 0.14 m/s). With the help of orbital maneuvers, it was possible to achieve not only a reduction in the rate of divergence of vehicles, but also their subsequent rapprochement.

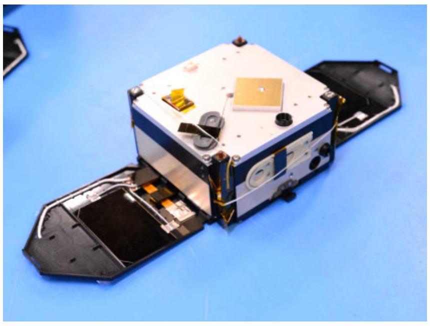

Рис. 4. Аппарат AeroCube-6 [19]

Fig. 4. AeroCube-6 spacecraft

Simulation of satellite orbital motion

To carry out the simulation, a freely available NASA software product: General Mission Analysis Tool (GMAT) is used in this work [20]. This software makes it possible to specify the state of the satellite in various forms of representation (in Cartesian coordinates and velocities, in the form of Keplerian elements, in spherical and geodetic coordinates) and perform numerical simulation of orbital motion in low-Earth orbit.

Calculations were carried out using the 89th order Runge-Kutta integration method with a variable time step in the range from 0.001 to 2700 s. The gravity model EGM-96 was used, taking into account higher spherical harmonics up to the tenth order. MSISE-90 with predicted values of solar and geomagnetic activity indices was chosen as the atmospheric model. In addition, the calculations take into account the disturbing influences of the gravitational effect of the Sun and Moon, as well as the pressure of solar radiation.

The simulation examines the dynamics of the inter-satellite distance of two CubeSat 3U vehicles weighing 4 kg, launched into a sun-synchronous orbit at an altitude of 567 km. According to the conditions, the satellites move in the same orbital plane with an inclination of 97.65°. During the launch phase, satellites are often put into orbit within a short period of time. During cluster startup, devices can start at intervals of 1–2 s. To ensure collision avoidance after launch, spacecraft are launched at different speeds, which leads to their orbits taking on different parameters. As a result, a satellite with a higher initial speed will be launched into a higher orbit. Moreover, it has a larger orbital period and will therefore lag behind the satellite with a lower initial speed. The simulated divergence rates of freely oriented spacecraft after insertion into orbit are shown in Fig. 5.

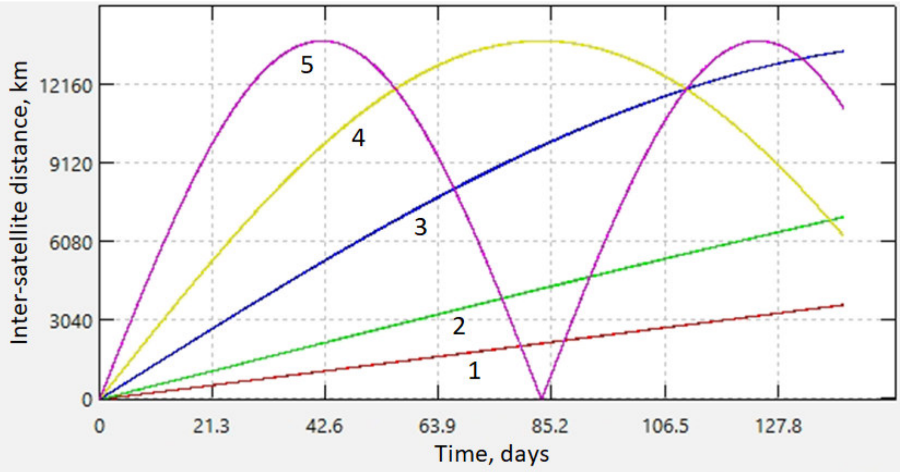

Рис. 5. Межспутниковое расстояние свободно ориентированных спутников
за 140 дней с начальной разностью скорости:
1 – 0,1 м/с; *2* – 0,2 м/с; *3* – 0,5 м/с; *4* – 1 м/с; *5* – 2 м/с

Fig. 5. The inter-satellite distance of freely oriented satellites in 140 days
with an initial velocity difference of:
1 – 0,1 m/s; *2* – 0,2 m/s; *3* – 0,5 m/s; *4* – 1 m/s; *5* – 2 m/s

According to the resulting graph, the divergence of satellites after launch is faster, if the difference in launch speeds is greater.

Over time, the satellites descend. At the same time, the density of the atmosphere increases unevenly (almost exponentially) with decreasing altitude, and the decrease in orbit accelerates, which leads to an increase in the difference in aerodynamic forces acting on satellites initially launched at different altitudes. As a result, the divergence accelerates. This process is facilitated by orbital disturbance factors. This effect is demonstrated in the graph of the orbital period versus time (Fig. 6).

In the graph above, the satellite with a higher initial speed is green, and the satellite with a lower initial speed is red. It is noticeable that the difference in the orbital periods of the spacecraft after launch increases with time, which indicates an acceleration of the divergence along the orbit.

Thus, the main criterion determining the possibility of using aerodynamic control to stabilize the relative position of satellites is the ability to equalize orbital periods within the allotted time. Below are the results of modeling the dynamics of satellites in the presence of aerodynamic control. A method for creating a differential force is being considered by transferring a vehicle launched into a lower orbit into a mode with minimal drag, orienting its end face in the direction of motion. In this case, it will have a midsection area equal to 100 cm^2, while the average midsection of a freely oriented satellite is 350 cm$^{2.}$

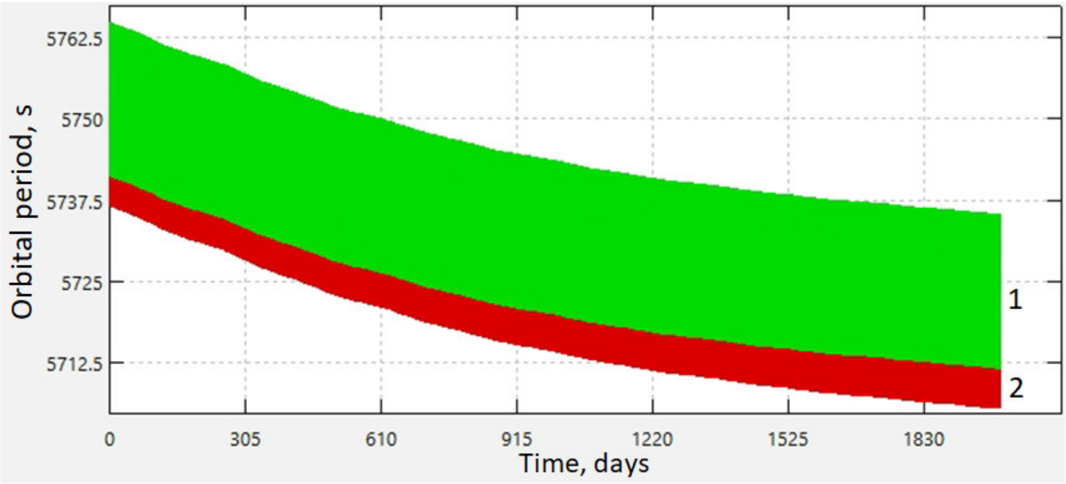

Рис. 6. Орбитальные периоды свободно ориентированных спутников
с разностью скоростей 2 м/с за 1500 дней:
1 – для спутника с большей начальной скоростью; *2* – для спутника с меньшей начальной скоростью

Fig. 6. Orbital periods of freely oriented satellites with a velocity difference of 2 m/s in 1500 days:
1 – for a satellite with a higher initial velocity; *2* – for a satellite with a lower initial velocity

Figure 7 shows the dynamics of the inter-satellite distance under the influence of differential force.

According to the schedule, within 12 days, aerodynamic control leads to stopping the process of divergence of satellites launched into orbit with a difference in launch speed of 0.1 m/s. The devices stop moving away due to the alignment of their orbital altitude. This is caused by a decrease in the rate of fall of a satellite released into a lower orbit as a result of its orientation to the state of least resistance.

To summarize, the limits of application of this management method were assessed. The ability to achieve stabilization of the relative motion of satellites was chosen as a criterion determining the feasibility of using aerodynamic control during a year. According to the simulation, this criterion is met for satellites launched into orbit with a difference in initial speed of up to 2 m/s (Fig. 8).

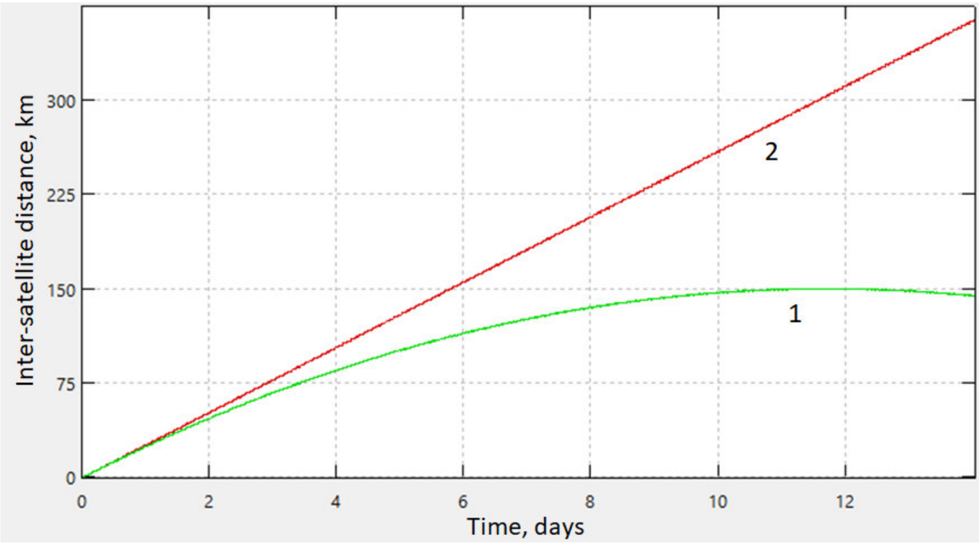

Рис. 7. Изменение межспутникового расстояния спутников с начальной разностью скорости 0,1 м/с:
1 – под действием аэродинамического управления; *2* – без управления

Fig. 7. Changing the inter-satellite distance of satellites with an initial velocity difference of 0.1 m/s:
1 – under the action of aerodynamic control; *2* – without control

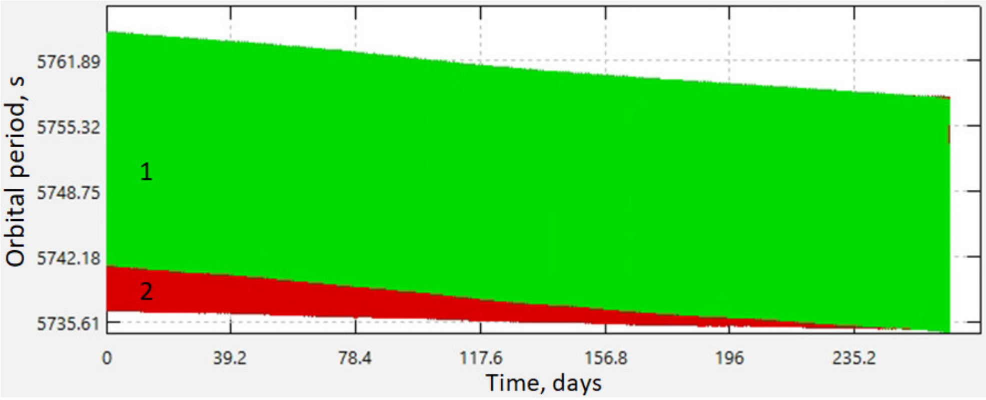

Рис. 8. Орбитальные периоды спутников под действием аэродинамического управления:
1 – для спутника с большей начальной скоростью; *2* – для спутника с меньшей начальной скоростью

Fig. 8. Orbital periods of satellites under the influence of aerodynamic control:
1 – for a satellite with a higher initial velocity; *2* – for a satellite with a lower initial velocity

Fig. 8 shows the dependence of orbital periods on time from the moment of satellite launch. Its alignment indicates stabilization of the relative motion of the spacecraft, which indicates the fundamental possibility of using aerodynamic control in these conditions. At the next stage of constructing the formation, it is necessary to perform an aerodynamic maneuver that brings the nanosatellites closer to a given distance, after which the orbital altitude must be equalized.

Conclusion

Small satellite systems enable to carry out an entirely new class of missions in navigation, communications, remote sensing and scientific research. Since individual spacecraft are limited by size, mass and power, commercially produced small satellites in large clusters can be useful in many scientific missions, such as gravity mapping, tracking forest fires, searching for water resources, etc. Creating a formation of satellites requires the use of a control device relative position of spacecraft.

This study simulates the distance dynamics between CubeSat nanosatellites launched into orbit at different launch speeds. Graphs of the inter-satellite distance are given under the condition of free orientation of the devices, as well as in the mode aerodynamic control. According to the simulation results, the aerodynamic differential force is applicable to construct a formation of nanosatellites of this class in a sun-synchronous orbit at an altitude of 570 km. This method can stabilize relative motion of satellites launched into orbit with a speed difference of up to up to 2 m/s per year.

To increase the capabilities of aerodynamic control, it is necessary to have a means of increasing the midsection of the spacecraft. It can be implemented in the form of deployable panels (solar panels). In the future, the results obtained are planned to be used to build the ReshUCube-3 space mission, within the framework of which several CubeSat devices with 1U and 3U form factors will be launched.

Библиографические ссылки

1. CubeSat [Электронный ресурс]. URL: https://www.cubesat.org (дата обращения: 25.01.2023).

2. A Review of Impending Small Satellite Formation Flying Missions / Bandyopadhyay S., Subramanian G., Foust R. и др. // 53rd AIAA Aerospace Sciences Meeting. Kissimmee. 2015. 17 p.

3. Hughes S. P. Preliminary Optimal Orbit Design for the Laser Interferometer Space Antenna (LISA) // Advances in the Astronautical Sciences. 2002. Vol. 111. P. 61–78.

4. Chung S., Miller, D., de Weck, O. ARGOS Testbed: Study of Multidisciplinary Challenges of Future Spaceborne Interferometric Arrays // Optical Engineering. 2004. Vol. 43, No. 9. P. 2156–2167.

5. Review of formation flying and constellation missions using nanosatellites / Bandyopadhyay S., Foust R., Subramanian G. et al. // Journal of Spacecraft and Rockets. 2016. Vol. 53 (3). 12 p.

6. Swarm-Keeping Strategies for Spacecraft Under J2 and Atmospheric Drag Perturbations / Morgan D., Chung S., Blackmore L. et al. // Journal of Guidance. Control, and Dynamics. 2012. Vol. 35, No. 5. P. 1492–1506.

7. Пантелеймонов И. Н. Перспективная методика управления полетом космических аппаратов одной орбитальной группировки с применением межспутниковых радиолиний // Ракетно-космическое приборостроение и информационные системы. 2018. No. 2. C. 73–83.

8. Horsley M. An investigation into using differential drag for controlling a formation of CubeSats // Advanced Maui Optical and Space Surveillance Technologies Conference. Maui, 2011. 18 p.

9. Иванов Д., Кушнирук М. Исследование алгоритма управления пространственным движением группы спутников с помощью аэродинамической силы // Препринты ИПМ им. М. В. Келдыша. 2017. № 53. С. 1–32.

10. Подъемная сила крыла самолета: формула [Электронный ресурс]. URL: https://travelsoul.ru/podemnaa-sila-kryla-samoleta-formula/ (дата обращения: 04.10.2023).

11. Vaughan W., Johnson D., Justus C. Guide to Reference and Standard Atmosphere Models : Tech. Rep. Reston : American Institute of Aeronautics and Astronautics, 2010. 142 p.

12. Jacchia L. New static models of the thermosphere and exosphere with empirical temperature profiles : Special Report. Cambridge : Smithsonian Astrophysical Observatory, 1970. 87 p.

13. Hedin A. Extension of the MSIS thermosphere model into the middle and lower atmosphere // J. Geophys. Res. 1991. No. 96. P. 1159–1172.

14. Picone J., Hedin A., Drob D. NRLMSISE00 empirical model of the atmosphere : Statistical comparisons and scientific issues // Journal of Geophysical Research. 2002. Vol. 107, No. A12. 16 p.

15. ГОСТ Р 25645.166-2004. Атмосфера Земли верхняя. Модель плотности для баллистического обеспечения полетов искусственных спутников Земли. М. : ИПК Издательство Стандартов. 2004. 24 с.

16. Harrison S. A free molecular aerodynamic investigation using multiple satellite analysis // Planet. Space Sci. 1996. Vol. 44, No. 2. P. 171–180.

17. Oltrogge D., Leveque K. An evaluation of cubesat orbit decay : Proceedings of 25th Annual AIAA/USU Conference on Small Satellites, Utah, 2011. 12 p.

18. Foster C., Hallam H., Mason J. Orbit Determination and Differential-drag Control of Planet Labs Cubesat Constellations // ArXiv : Space Physics. 2015, 13 p.

19. Gangestad J., Rowen D., Hardy B. Flight Results from AeroCube-6: A Radiation Dosimeter Mission in the 0.5U Form Factor // CubeSat Developers' Workshop. San Luis Obispo. 2016. 18 p.

20. General Mission Analysis Tool (GMAT) v.R2016a [Электронный ресурс]. URL: https://software.nasa.gov/software/GSC-17177-1 (дата обращения: 08.02.2023).

References

1. CubeSat. Available at: https://www.cubesat.org (accessed 25.1.2023).

2. Bandyopadhyay S., Subramanian G., Foust R., Hadaegh F. A Review of Impending Small Satellite Formation Flying Missions. *53rd AIAA Aerospace Sciences Meeting*, Kissimmee, 2015, 17 p.

3. Hughes S. P. Preliminary Optimal Orbit Design for the Laser Interferometer Space Antenna (LISA). *Advances in the Astronautical Sciences*, 2002, vol. 111, p. 61–78.

4. Chung S., Miller, D., de Weck, O. ARGOS Testbed: Study of Multidisciplinary Challenges of Future Spaceborne Interferometric Arrays. *Optical Engineering*, 2004, vol. 43, no. 9, p. 2156–2167.

5. Bandyopadhyay S., Foust R., Subramanian G., Chung S., Hadaegh F. Review of formation flying and constellation missions using nanosatellites. *Journal of Spacecraft and Rockets*, 2016, vol. 53 (3), 12 p.

6. Morgan D., Chung S., Blackmore L., Acıkmese B., Bayard D., Hadaegh F. Swarm-Keeping Strategies for Spacecraft Under J2 and Atmospheric Drag Perturbations. *Journal of Guidance, Control, and Dynamics*, 2012, vol. 35, no. 5, p. 1492–1506.

7. Panteleimonov I. N. *Perspektivnaya metodika upravleniya poletom kosmicheskikh apparatov odnoi orbital'noi gruppirovki s primeneniem mezhsputnikovykh radiolinii* [A promising technique for controlling the flight of spacecraft of one orbital grouping using inter-satellite radio lines]. *Raketno-kosmicheskoe priborostroenie i informatsionnye sistemy*. 2018, no. 2, p. 73–83 (In Russ.).

8. Horsley M. An investigation into using differential drag for controlling a formation of CubeSats. *AMOS Technologies Conference*, Maui, 2011, 18 p.

9. Ivanov D., Kushniruk M. *Issledovanie algoritma upravleniya prostranstvennym dvizheniem gruppy sputnikov s pomoshch'yu aerodinamicheskoi sily* [Investigation of Control Algorithm Using Aerodynamic Force for Satellite Formation Flying Three-Dimensional Motion]. *Preprinty IPM im. M. V. Keldysha*. 2017, no. 53, p. 1–32.

10. *Pod"emnaya sila kryla samoleta: formula* [Lifting force of a winged aircraft: formula]. Available at: https://travelsoul.ru/podemnaa-sila-kryla-samoleta-formula/ (accessed 04.10.2023).

11. Vaughan W., Johnson D., Justus C. Guide to Reference and Standard Atmosphere Models : Tech. Rep. Reston, American Institute of Aeronautics and Astronautics Publ., 2010, 142 p.

12. Jacchia L. New static models of the thermosphere and exosphere with empirical temperature profiles. Special Report. Cambridge, Smithsonian Astrophysical Observatory, 1970, 87 p.

13. Hedin A. Extension of the MSIS thermosphere model into the middle and lower atmosphere. *Journal of Geophysical Research*, 1991, no. 96, p. 1159–1172.

14. Picone J., Hedin A., Drob D. NRLMSISE00 empirical model of the atmosphere : Statistical comparisons and scientific issues. *Journal of Geophysical Research*, 2002, vol, 107, no. A12, 16 p.

15. GOST R 25645.166–2004. Atmosfera Zemli verkhnyaya. Model' plotnosti dlya ballisticheskogo obespecheniya poletov iskusstvennykh sputnikov Zemli. [State Standard R 25645.166–2004. Earth upper atmosphere. Density model for ballistic support of flights of artificial earth satellites]. Moscow, IPK Izdatelstvo standartov Publ., 2004. 24 p.

16. Harrison S. A free molecular aerodynamic investigation using multiple satellite analysis. *Planet. Space Sci*., 1996, vol. 44, no. 2, p. 171–180.

17. Oltrogge D., Leveque K. An evaluation of cubesat orbit decay. *Proceedings of 25th Annual AIAA/USU Conference on Small Satellites*, Utah, 2011, 12 p.

18. Foster C., Hallam H., Mason J. Orbit Determination and Differential-drag Control of Planet Labs Cubesat Constellations. *ArXiv : Space Physics*, 2015, 13 p.

19. Gangestad J., Rowen D., Hardy B. Flight Results from AeroCube-6: A Radiation Dosimeter Mission in the 0.5U Form Factor. *CubeSat Developers' Workshop*, San Luis Obispo, 2016, 18 p.

20. General Mission Analysis Tool (GMAT) v.R2016a. Available at: https://software.nasa.gov/software/GSC-17177-1 (accessed: 08.2.2023).

Лукьянов Михаил Михайлович – бакалавр; Сибирский государственный университет науки и технологий имени академика М. Ф. Решетнева. E-mail: mishka.1255555@mail.ru.

Зуев Дмитрий Михайлович – старший преподаватель кафедры технической физики, инженер научно-производственной лаборатории «Малые космические аппараты»; Сибирский государственный университет науки и технологий имени академика М. Ф. Решетнева. E-mail: zuevdmitriy93@yandex.ru.

Lukyanov Mikhail Mikhailovich – Bachelor; Reshetnev Siberian State University of Science and Technology. E-mail: mishka.1255555@mail.ru.

Zuev Dmitrii Mikhailovich – Senior Lecturer of Applied Physics Department, Engineer of Small Satellites Laboratory; Reshetnev Siberian State University of Science and Technology. E-mail: zuevdmitriy93@yandex.ru.